SEISMIC ZONATION IN TERMS OF ARRAY OBSERVATION DATA

Kei TANII[1] and Makoto KAMIYAMA[2]

SUMMARY

Surveys of P and S waves' velocities of sedimentary layers are necessary to develop the seismic zonation of an area. The so-called P to S wave, which is originated at the interface of sedimentary layers converting from P wave to S wave, is effective for such surveys. Especially, the PS-P time defined as the difference in arrival times between P to S wave and direct P wave is important for surveys of deep deposits because it depends only on velocity structures of sedimentary layers overlying the seismic bedrock. The purpose of this paper is to apply the PS-P time to seismic zonation using earthquake-motion records by an array observation system. The array observation system here was installed in Sendai City, Japan in 1997 and has observed more than 200 earthquake-records. The system, named Small-Titan, is the "local laboratory array" composed of 20 observation stations. In addition to the array stations, the MYGH01 observation site of KiK-net, where a vertical array of the depth of about 1200m has been deployed with full geophysical-information of P and S waves' velocities near Small-Titan, was also used to calibrate PS-P time data from Small-Titan. We used a combination of two methods such as the receiver function and complex envelope to exactly detect PS-P times. Both methods were applied to the radial and vertical components in the initial parts of motions. The analyses for the vertical observation site at MYGH01 confirmed the accuracy of the PS-P times estimated by both methods. This confirmation led to the estimates of PS-P times at 20 observation stations of Small-Titan and mapping of PS-P times' distribution in Sendai City. The zoning map of PS-P time showed a good correlation with empirical zoning map of seismic intensity in Sendai City.

INTRODUCTION

It is known that seismic ground motions are strongly affected by deep underground structures as well as surface soils. It is important to consider the structure of sedimentary layers overlying seismic bedrock to perform the seismic zoning. Especially, surveys for P wave and S wave velocity structures of sedimentary layers are necessary to develope the seismic zoning. The P-to-S-converted waves originated at sedimentary layer's interfaces are effective for such a survey. The difference in arrival times between P to S converted waves and direct P waves, that is, the PS-P time depends only on velocity structures of sedimentary layers overlying the seismic bedrock. Thus, the PS-P time could lead to a key parameter for the seismic zoning.

---

[1] Ph.D Condidate, Tohoku Institute of Technology, Sendai, JAPAN. Email:keitanii@smail.tohtech.ac.jp
[2] Professor, Tohoku Institute of Technology, Sendai, JAPAN. Email:mkamiyam@tohtech.ac.jp

This study investigates the applicability of the receiver function method proposed by Langston [1] to detect the PS-P time from strong motion records observed by an array system. The receiver function is obtained by the Fourier inverse transform of spectral ratio function of horizontal to vertical components in the initial part of motions. This study also compares the receiver function with the complex envelope. In addition, the difference in rising time between horizontal and vertical components of the complex envelope is used to detect the PS-P time, because the complex envelope is more effective for visual interpretation than the original signals of motions.

We first estimate the PS-P time for the MYGH01 observation site of the digital strong-motion seismograph KiK-net, which has been deployed by the National Research Institute for Earth Science and Disaster Prevention. Furthermore, we theoretically compute PS-P time at the MYGH01 observation site of KiK-net using the information of P and S waves' structures obtained by PS-well logging and compare the theoretical PS-P time with the ones estimated based on motion records. We make such a comparison to confirm the validity of the PS-P time estimates due to both the receiver function and the complex envelope methods.

We applied our methods of the PS-P time estimate to observed strong-motion records by an array observation system. The system, named Small-Titan, was installed in Sendai City, Japan in 1997. It consists of 20 observation sites that are deployed at various kinds of ground structures to effectively detect local site conditions. Small-Titan has obtained records due to a total of 250 earthquakes as of Feb. 20, 2004, enabling to construct an empirical map of seismic zoning.

Next, we relate the PS-P time at the MYGH01 observation site of KiK-net with the one estimated at the ARAH observation site of Small-Titan to investigate whether or not the velocity structures of sedimentary layers under both sites are similar to each other because the two sites are relatively close with a distance of about 3 km.

Finally we estimate the PS-P times at all the 20 sites of Small-Titan to correlate them with the zoning map of seismic intensity that was empirically derived from observed ground motions.

OBSERVATION SYSTEM

Figure 1 shows the layout of the Small-Titan observation sites with a digital elevation in Sendai City. As shown in Figure 1, the city area is roughly divided into two categories of geology by a clear line of the lowest elevation running from southwest to northeast : the northwest area across the line consists of diluvial deposits while the southeast part is covered by alluvial sediments. The observation stations were deployed taking the following points into account:

(1) The Sendai City region was covered as evenly as possible so as to give greater efficiency in applying the observation system to the disaster mitigation system.

(2) Various kinds of soils were selected so that the local site effects on seismic motions could be effectively detected.

(3) Man-made lands that had been developed for housing lots were included as an observation site based on the damage experience due to the Miyagi-ken-oki Earthquake in 1978.

(4) The observation sites were deployed to detect systematically the effect of laterally inhomogeneous soils on ground motions. Namely, the linear cross sections along the several observation sites provide a typical structure of laterally inhomogeneous ground.

(5) The Nagamachi-Rifu Fault recently has been causing small earthquakes that may be considered to be pre-earthquakes for a possible large earthquake in the future. If the fault triggers such a large earthquake, the observation sites here enable to detect various source effects such as the radiation pattern, directivity, inhomogencity of faulting and so on.

In developing an observation system characterized as the simple extended array, its most important strategy is to select a site as an appropriate reference site so that the amplification factors at each site can be effectively estimated. In this observation system, the SHOK site was selected to meet the reference site
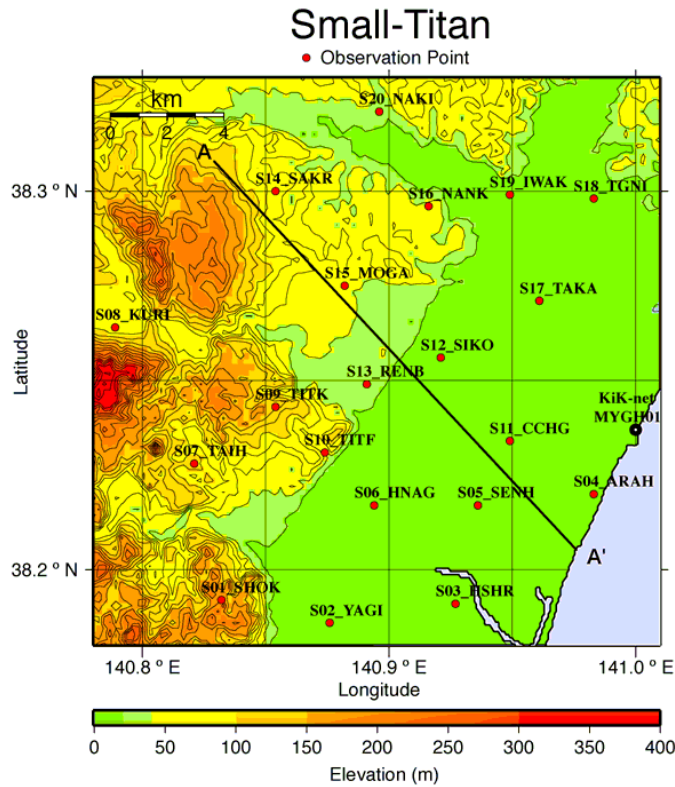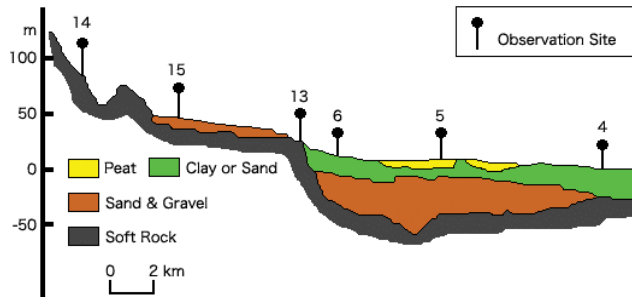
Figure 1: Observation site layout and topography

Figure 2: Typical geologic profile (A-A' in Fig. 1)

condition on account that it lies on the outcrop consisting of the andesite deposit, called the Takadate Layer. According to geological surveys, the layer is considered to deposit at a depth of about 500m in the central part of Sendai City.

In summary, the observation sites are classified in terms of soil types as follows:

Bed rock: SHOK

Diluvial plateau: TAIH, KURI, TITK, TITF, SAKR, MOGA, NANK and NAKI

Alluvial lowland: YAGI, HSHR, ARAH, SENH, HNAG, CCHG, SIKO, TAKA and TGNI

Diluvium-alluvium boundary: TITF, RENB and IWAK

Man-made land: TAIH, TITK and NANK

Alluvial soft soils: SENH and TGNI

Figure 2 shows a typical example of geologic profile along a cross section line normal to the Nagamachi-Rifu Fault together with the corresponding observation sites. It can be seen from Figure 2 that Small-Titan was designed with due consideration toward the effect of lateral inhomogeneous soils on ground motions.

Figure 1 also shows the MYGH01 observation site of KiK-net, located in the neighborhood of the S04_ARAH site of the Small-Titan system. At each observation site of Small-Titan, soil conditions are available within surface layers, but we have almost no information about ground structures at deep deposits down to the seismic bedrock. The MYGH01 site of KiK-net that constitutes a vertical array of observation, on the other hand, has full geophysical information of P and S waves' velocities until a depth of about 1206m. Therefore, we used the MYGH01 site as reference for the geophysical surveys of the Small-Titan sites in light of the fact that it is relatively close to the ARAH site of Small-Titan.

EMPIRICAL SEISMIC ZONATION WITH AID OF OBSERVED MOTIONS

Figure 3 shows a map of seismic intensity empirically derived from observed ground motions by Small-Titan. As is well known, there are a number of parameters representing the intensity of motions such as peak acceleration, but the so-called seismic intensity might be the most appropriate parameter because of its overall effects on earthquake damage. Especially, seismic intensity is determined instrumentally in Japan using motion records so that it represents a reliable engineering parameter. We obtained seismic intensities at the Small-Titan sites using motion records observed during about 40 different types of earthquakes. Then these values of seismic intensity were dealt with statistically to get an average feature

of relative intensity. Figure 3 is a map drawn to relatively present seismic intensity in Sendai City. In Figure 3, the warm color areas indicate relatively larger intensities while the cool color areas correspond to smaller intensities. Comparisons between Figure 1 and Figure 3 indicate two interesting things. First, the distribution of intensity in Figure 3 has a high correlation with the elevation map in Figure 1 : the high seismic intensity areas generally fall in the lowland of alluvial sediments whereas the low seismic intensities lie in the high elevation of diluvial deposits. This might reflect the difference of surface soils in both areas, suggesting that the alluvial sediments amplify ground motions. However, a close look at the distribution of seismic intensity within the high elevation area clarifies the second point of the interesting features. That is, a part including several sites such as S07_TAIH, S10_TITF, S09_TITK and S08_KURI within the high elevation area clearly shows slightly higher seismic intensity compared with other sites within

Figure 3: Empirical zoning map of seismic intensity

the area. This distribution of seismic intensity within the high elevation area can not be explained by its surface soils. Therefore, it is natural to consider that other reasons except for the surface soils bring about such a distinctive distribution of seismic intensity within the high elevation area.
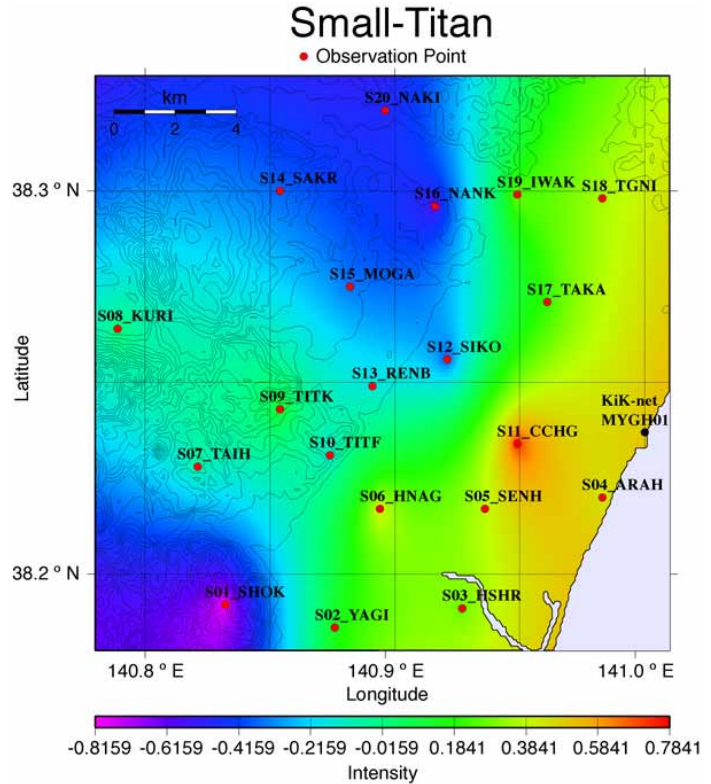

ESTIMATES OF THE PS-P TIME

Analysis of the receiver function

Figure 4 shows a flow chart to obtain the receiver function using observed motions of three components. The flow consists of five steps. Details of each step are :

Suppose in the flow that the target components of analysis are the radial and vertical components. We assume that the radial and vertical components of motions represent respectively the horizontal and vertical components of SV wave propagating from the hypocenter to the observation site. Note that the radial direction here is simply determined by the line connecting the hypocenter with the observation site. We synthesize the observed motions, which are obtained in the three directions of north-to-south (NS), east-to-west (EW) and up-to-down (UD), to provide the radial and transverse components of motions.

Step 2 is to set an analysis section for the initial part of each component of motions. For such a purpose, we applied a time window illustrated in Figure 4 to the original motions. The time window has a cosine-type filter at its end to taper the later motions. This cosine-tapered time window makes it possible to focus our analysis on the motion parts composed mainly of P-to-S converted waves due to layers' interfaces. The values of te and α of the time window depend on the underground structure in question : te and α are uniformly set to be 1.0-2.0 sec and 0.2-1.0 sec, respectively, in reference to the supposed structures at our objective sites.
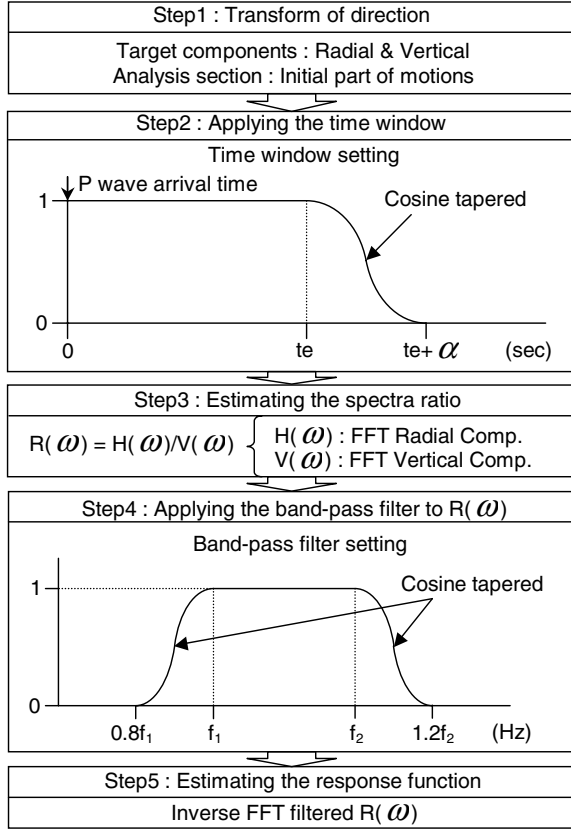
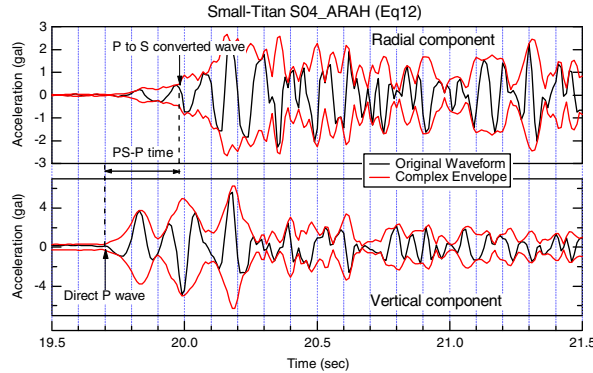**Figure 4: Workflow of the receiver function**

Figure 5: Observed record and its complex envelope

Step 3 is to obtain the spectra ratio of the radial component by the vertical component. This process is equivalent to the deconvolution of the vertical motions from the radial motions. We carry out the process by making the FFT analysis for both motions filtered by the time window.

A band-pass filter is applied to the spectra ratio in step 4 to remove some noises in both the high and low frequencies. As shown in Figure 4, the band-pass filter has a cosine taper at the ends of the highest and lowest frequencies to make its operation smooth. The constants of f_1 and f_2 for the filter are given uniformly to be 1 Hz and 5-10Hz, respectively.

Step 5 is to inversely transform the filtered spectra ratio from the frequency domain to the time domain. Through this process, we expect to detect the rise times of various waves such as P-to-S converted wave.

Analysis of the complex envelope

n addition to the receiver function analysis, we reinforced our analysis by obtaining the complex envelope for the radial and vertical motions. The "Complex Envelope" of motions was first proposed by Farnbach [2] and has been used for various kinds of applications in earthquake engineering. The complex envelope is defined as an imaginary number system in which the real part consists of a time history while the imaginary part stems from the histories' Hilbert transform. These real part and imaginary parts of the complex envelope represent some physical characters of motions, especially the absolute values of both parts provide literally a kind of envelope for the original time history. Such an envelope derived by the complex envelope enables to detect the rising time of phases equivalent to the arrival of some wave, for example P-to-S converted wave. With aid of its effect, we made the complex envelope analysis to the radial and vertical motions after processing of the same time-window as the receiver function analysis. One example of such an envelope analysis is shown in Figure 5 together with the original waveforms of radial and vertical motions. In this figure, the rising times for the direct P wave and P-to-S converted wave are given along with an estimated PS-P time. As shown in Figure 5, the introduction of the complex envelope makes it easier to identify some phases of a wavetrain with less ambiguity than the wavetrain itself. Furthermore, the ratio between the complex envelope of the radial and vertical components, abbreviated as H/V, might provide additional meanings involved in their original wavetrains because SV wave travels with a distinctive feature of H/V. So, we also carry out the H/V analysis based on the complex envelope technique.

EARTHQUAKE CONDITIONS FOR ANALYSIS

As described in the preceding section, Small-Titan obtained records for a total of 250 earthquakes as of Feb. 20, 2004. Similarly, the MYGH01 site of KiK-net observed almost the same number of records. In this study, we selected earthquakes that simultaneously triggered all the 20 sites of Small-Titan and the MYGH01 site. The epicenters of these earthquakes are shown in Figure 6. We carried out the receiver function analysis and complex envelope analysis for the radial and vertical records due to these earthquakes. Both results of the receiver function and complex envelope were normalized by the maximum amplitude for each analysis and then averaged over the representative earthquakes : Eq07, Eq12, Eq13, Eq1X, Eq14, Eq20, Eq21 and Eq27. This average operation aimed at removing various kinds of noises resulting from causes such as instrumental technique.

Figure 6: A map of earthquake locations

EXAMPLE OF ANALYZED RESULTS

Analyzed results for the MYGH01 site of KiK-net

Analyzed results for the MYGH01 site of KiK-net are first exemplified. Figure 7 shows from the top : (a) receiver function results obtained by two types of band-pass filter – from 1Hz to 5Hz and from 1Hz to 10Hz ; (b) H/V result of complex envelope ; (c) complex envelopes of the radial and vertical components ; (d) travel-time curves theoretically estimated for the PS waves' structure at the MYGH01 site and (e) complex envelopes of the radial and vertical components of the records obtained at the downhole site of a depth of 1206m. Each figure in Figure 7 has a time axis measured from the arrival time of direct P wave. Note that the MYGH01 site is a vertical array system of observation and the 3 upper figures from the top indicate the results for the ground surface site while the lowest figure at the bottom is for the downhole site.

The receiver functions in Figure 7(a) fluctuate in time, but show a peak around a time of 0.385 sec for both band-pass filter. This time almost agrees with a time identified by the other results of analysis ; that is, the main rising time of H/V result in the (b) figure, the distinctive rising time of complex envelope for the radial component in the (c) figure and the theoretical arrival time for the P-to-S converted wave at the interface of a depth of 648m in the (d) figure. There is a clear difference in the complex envelopes between the radial and vertical components in the figure (c). The vertical component prevails in an early stage of time immediately after the P wave's arrival, meaning that P wave mainly travels during the time stage. As opposed to such an early prevalence of the vertical component, the radial component rises rapidly at a time of about 0.385 sec and becomes prevalent until almost the same level of the vertical component. This suggests that SV wave arrived at the rising time on the ground surface, as a form converted from P wave to S wave at an underground interface. Therefore, the PS-P time related with the interface at a depth of 648m is judged to be 0.385 sec. This judgement based on the observation of ground motions is compatible to the theoretical estimate shown in Figure 7(d). On the other hand, both complex
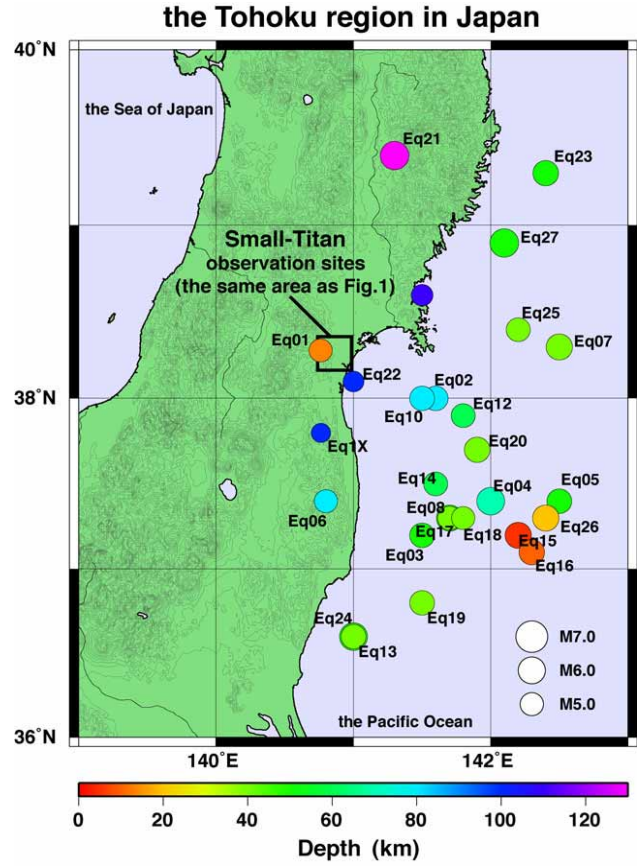
Figure 7: Result for KiKnet MYGH01

Figure 8: Comparisons of results between MYGH01 and S04_ARAH

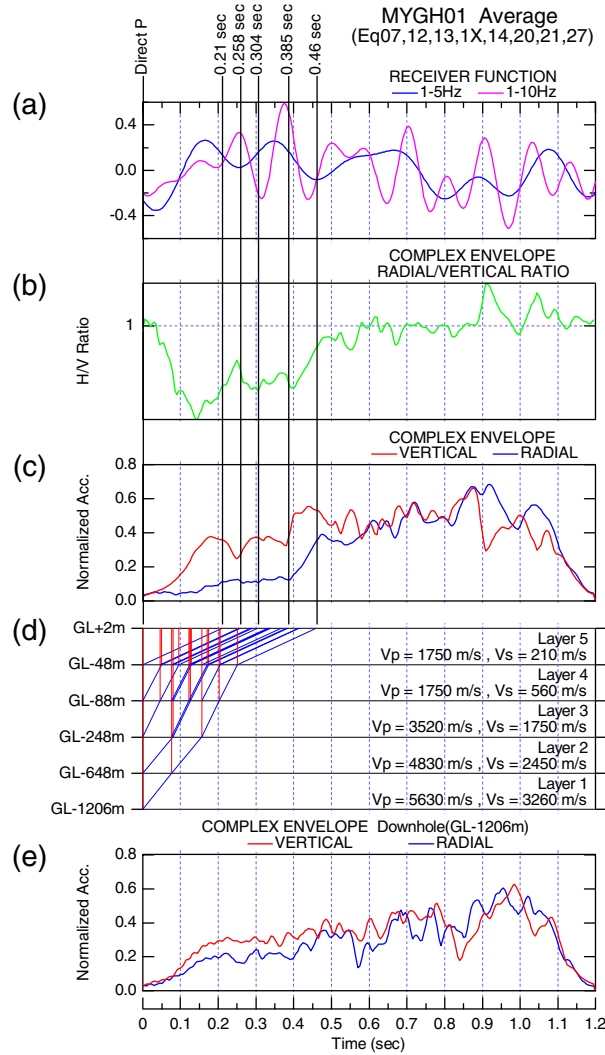**Figure 9: Result for S02_YAGI**

envelopes at the downhole site in Figure 7(e) differ little between the radial and vertical components from the P-wave arrival, indicating that there is almost no converted waves at such a depth.

Comparisons of analyzed results between the MYGH01 site of KiK-net and the ARAH site of Small-Titan

Following the analyses for the MYGH01 site of KiK-net, we compared them with the results analyzed for the ARAH site of Small-Titan. As shown in Figure 1, both sites are situated closely to each other so that they might provide similar results. Figure 8 shows from the top : (a) results of receiver function ; (b) H/V of complex envelopes and (c) complex envelopes of the radial and vertical
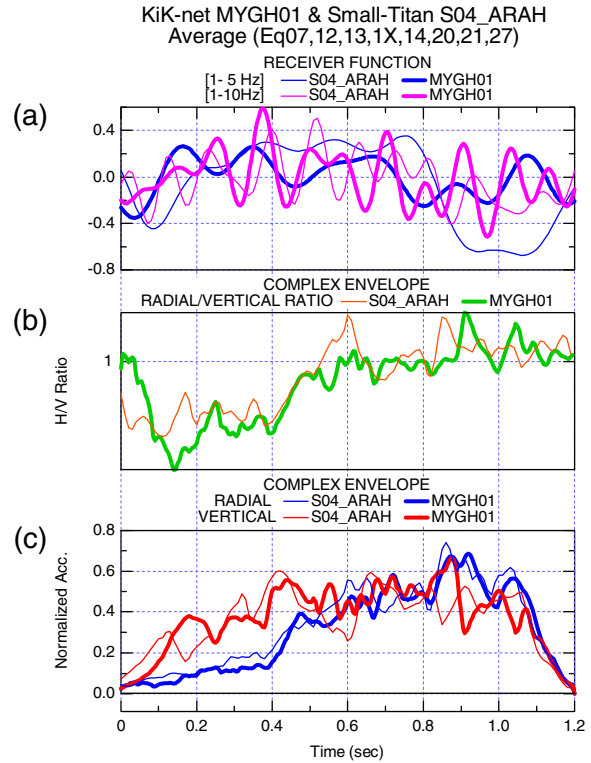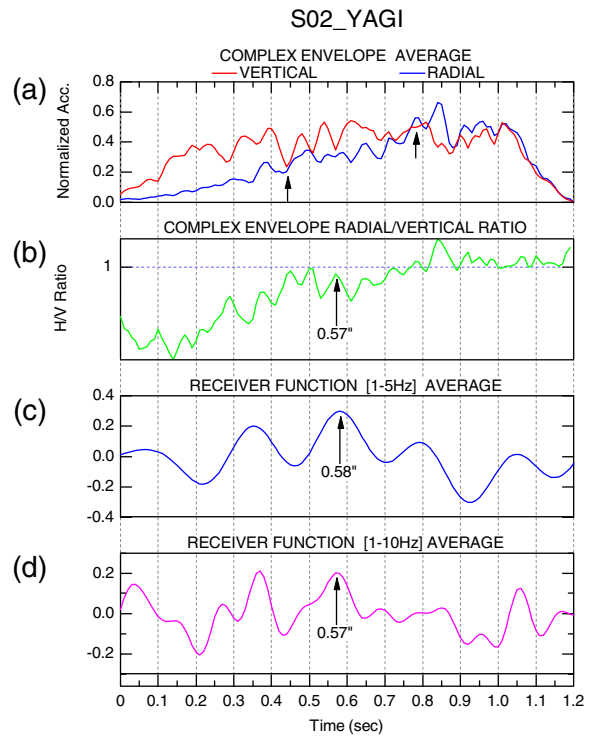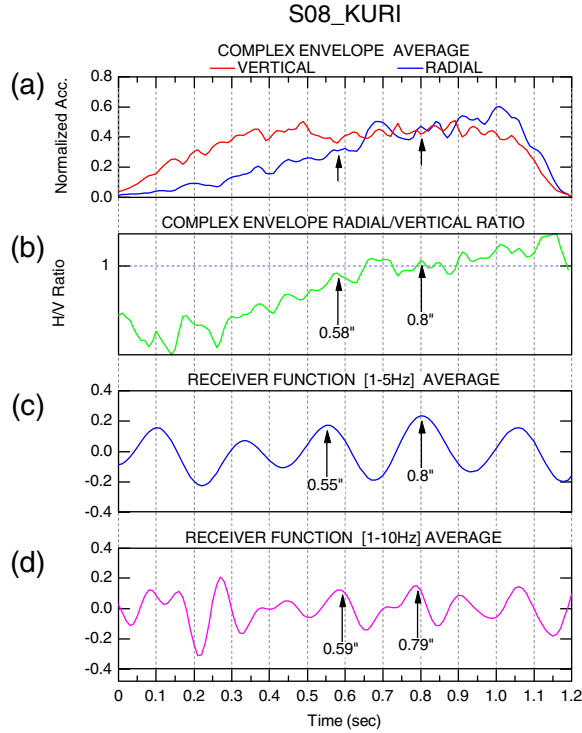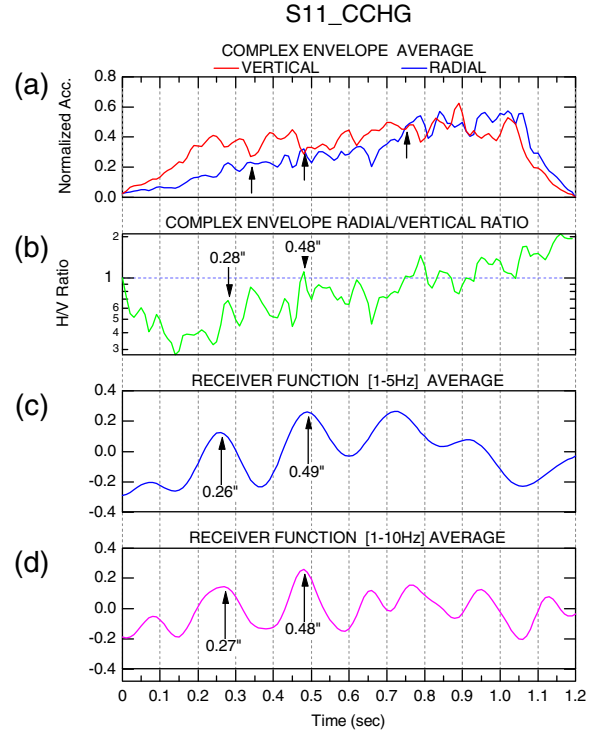
Figure 10: Result for S08_KURI

Figure 11: Result for S11_CCHG

components for the MYGH01 site and the ARAH site. Each comparison in Figure 8 reveals little difference between both sites, suggesting almost the same PS-P time for them. Accordingly, the ARAH site may have almost the same ground structure as the one at the MYGH01 site, especially the conspicuous interface of layer at a depth of 648m.

Analyzed results for the observation sites of Small-Titan
The results analyzed for the MYGH01 site and the ARAH site demonstrate that our combination analyses of receiver function and complex envelope are encouraging, so we proceeded our analysis to all the sites of Small-Titan. Three examples of analyzed results among all the sites are shown in Figures 9, 10 and 11, respectively for the S02_YAGI site, S08_KURI site and S11_CCHG site. These figures are all composed of 4 sub-figures : (a) complex envelopes of the radial and vertical components ; (b) H/V of complex envelopes ; (c) receiver function due to a 1-5Hz band-pass filter and (d) receiver function due to a 1-10Hz band-pass filter. In these sub-figures, some arrows are plotted with a number to identify rising times of P-to-S converted waves. Unfortunately, it is impossible to identify an unique rising time in these sub-figures, indicating that there are several conspicuous interfaces of layers to strongly convert P wave to S wave at these sites.

DISCUSSION AND ZONING OF DEPTH OF SEISMIC BEDROCK

In the foregoing sections, PS-P times at each site of KiK-net and Small-Titan were obtained by the receiver function technique and complex envelope method so as to have several values. Related with the characteristic distribution of seismic intensity in the high elevation area of Figure 3, however, we focused our main interest on the deepest interface equivalent to the 648m-depth layer at the MYGH01 site. In order to determine the PS-P time related with the layer, which is called here the bedrock, at each observation site of Small-Titan, we obtained the maximum PS-P time based on some overall judgements of the sub-figures. Such maximum PS-P times equivalent to the depth of the bedrock are mapped and
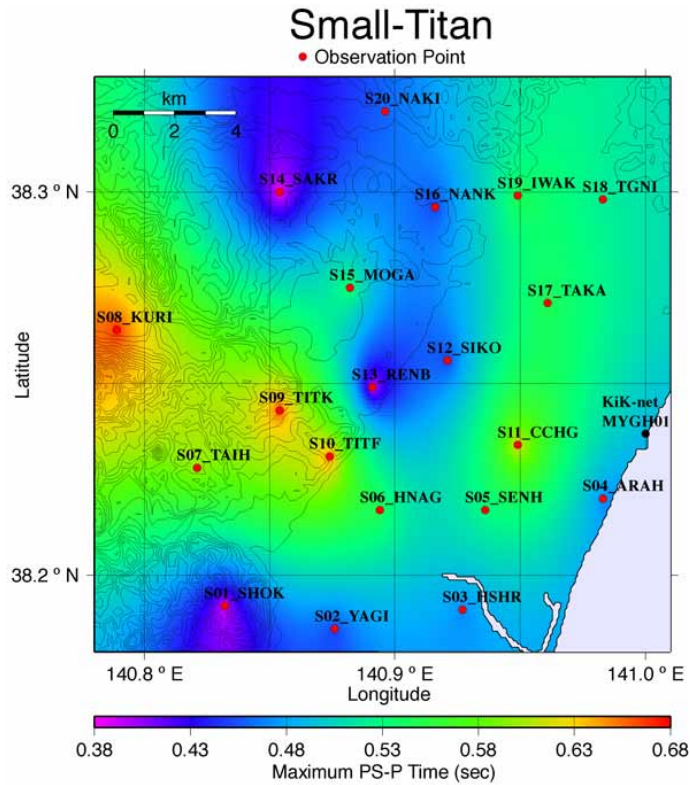
Figure 12: The zoning map of maximum PS-P time

displayed in Figure 12. Comparisons between Figure 3 and Figure 12 show a relatively good correlation between them, in particular, revealing that the large PS-P time area including the observation sites like S07_TAIH, S08_KURI, S09_TITK and S10_TITF in Figure 12 coincide almost with the high seismic intensity area including the same sites in Figure 3.

CONCLUDING REMARKS

The simultaneous analyses of receiver function and complex envelope are very effective for estimating the PS-P time. The analyses were applied to observed records by Small-Titan and KiK-net. The former records resulted from 20 observation sites composed of various soils while the latter records are from a vertical array of the depth of 1206m. The Small-Titan system obtained empirically a map of seismic zonation in terms of seismic intensity, showing a distinctive distribution reflecting local site conditions. In order to investigate such a distribution of intensity in connection to PS-P times at each site of Small-Titan, we analyzed the observed records of Small-Titan by receiver function and complex envelope. At the same time, the observed records at the vertical array site of KiK-net, which has a geophysical information and is located closely to an observation site of Small-Titan, were used as reference to calibrate the accuracy of analysis. As a result, we obtained the maximum PS-P times at each site of Small-Titan related with the depth of the bedrock in Sendai City area. It is finally concluded that the distinctive distribution of seismic intensity in the Sendai City area has a strong correlation with the depth of the bedrock as well as the surface soil conditions divided roughly into the diluvial deposits and alluvial sediments.

ACKNOWLEDGEMENTS

REFERENCES

1. Charles A. Langston "Structure Under Mount Rainier, Washington, Inferred From Teleseismic Body Waves" Journal of Geophysical Research, Vol.84, No.B9 (1979), pp.4749-4762.
2. John S. Farnbach "THE COMPLEX ENVELOPE IN SEISMIC SIGNAL ANALYSIS" Bulletin of the Seismological Society of America, Vol.65, No.4, pp.951-962.1975.

3. Yuichi S, Makoto K. "A high-density array observation system small-titan : an instroduction and it's strong-motion records". Proceedings of the 12th World Conference on Earthquake Engineering, Auckland, New Zealand. Paper no. 1469. 2000.
4. Kikuji K, Tomiichi U, Mitsugu M, Hiroyoshi K. "AN INVESTIGATION ON DETECTION METHOD OF P TO S CONVERTED WAVES FOR ESTIMATING DEEP UNDERGROUND STRUCTURES" J. Struct. Constr. Eng., AIJ, No. 505, 45-52, Mar., 1998.